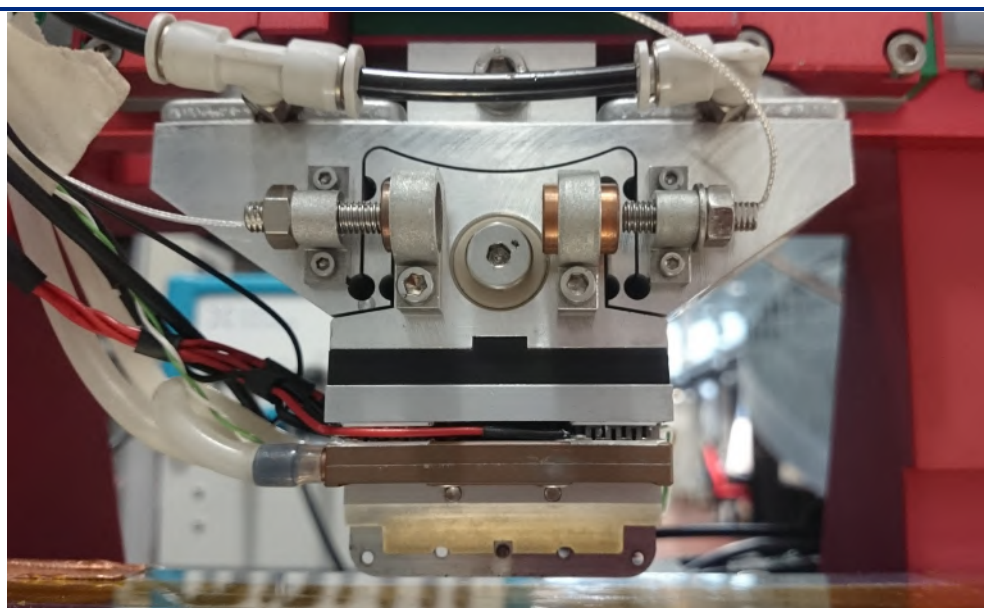




---

# Friction of ice during ice skating



THESIS

submitted in partial fulfillment of the  
requirements for the degree of

MASTER OF SCIENCE

in

PHYSICS

|                             |                             |
|-----------------------------|-----------------------------|
| Author :                    | Charlotte Jansen            |
| Student ID :                | 1241257                     |
| Supervisor :                | Prof.dr.ir. T.H. Oosterkamp |
| 2 <sup>nd</sup> corrector : | Dr.ir. S.J. van der Molen   |

Leiden, The Netherlands, October 6, 2017



# Friction of ice during ice skating

**Charlotte Jansen**

Huygens-Kamerlingh Onnes Laboratory, Leiden University  
P.O. Box 9500, 2300 RA Leiden, The Netherlands

October 6, 2017

## **Abstract**

A hinge specifically designed for continuous friction measurements during ice skating was tested and used. The hinge can handle large vertical normal forces to simulate the weight of a real person on a skate, and is very flexible in the horizontal direction, so it deforms under a friction force. Two sensors on the hinge measure the deformation. Friction measurements were done with a part of a real skate, with varying temperatures, skating speeds and normal forces on the skate. A clear dependence of friction on temperature was found. Friction coefficients for an ice temperature of  $-20^{\circ}\text{C}$  and air temperature of  $-10^{\circ}\text{C}$  varied between 0.04 and 0.1, and coefficients for an ice temperature of  $-10^{\circ}\text{C}$  and air temperature of  $-6^{\circ}\text{C}$  varied from 0.006 to 0.016. The temperature of the skate was held at  $-10^{\circ}\text{C}$  for both cases. The results also suggest friction dependence on skating speed and normal force, but this has to be verified. During the calibration of the setup it was found that the vertical force, controlled by air pressure, could be determined up to a factor of 2. Furthermore there was a large variation (up to a factor 2) in friction coefficients from measurements under the same circumstances, on the same ice layer. These could have been caused by changing humidity in the setup, as this was not monitored during the measurements. The setup works, but needs to be improved for more precise friction measurements. A humidity sensor in the setup is recommended.



# Contents

|          |  |           |
|----------|--|-----------|
| <b>1</b> | <b>Introduction</b>                      | <b>1</b>  |
| <b>2</b> | <b>Previous work</b>                     | <b>3</b>  |
| 2.1      | Theory                                   | 3         |
| 2.1.1    | Water layer                              | 3         |
| 2.1.2    | Other theories                           | 4         |
| 2.2      | Previous research                        | 5         |
| <b>3</b> | <b>Setup</b>                             | <b>9</b>  |
| 3.1      | General                                  | 9         |
| 3.1.1    | The ice                                  | 9         |
| 3.1.2    | The skate                                | 10        |
| 3.1.3    | Water layer measurements setup           | 10        |
| 3.2      | Setup: environmental & skating controls  | 11        |
| 3.2.1    | Temperature controls                     | 11        |
| 3.2.2    | Motor                                    | 13        |
| 3.2.3    | Vertical force                           | 14        |
| 3.3      | Friction measurements setup              | 17        |
| 3.3.1    | Hinge                                    | 17        |
| 3.3.2    | Sensors                                  | 18        |
| 3.3.3    | Calibration of the hinge                 | 20        |
| 3.3.4    | Friction measurements methods            | 23        |
| <b>4</b> | <b>Results and discussion</b>            | <b>25</b> |
| 4.1      | Friction on teflon                       | 25        |
| 4.2      | Time dependence                          | 26        |
| 4.3      | Space dependence                         | 30        |
| 4.4      | Height profile measurement after skating | 30        |

---

|          |   |           |
|----------|---|-----------|
| 4.5      | Speed dependence                                | 33        |
| 4.6      | Temperature dependence                          | 33        |
| 4.7      | Coefficient of friction                         | 35        |
| 4.7.1    | Normal force dependence                         | 36        |
| 4.8      | Humidity dependence?                            | 38        |
| <b>5</b> | <b>Conclusions &amp; outlook</b>                | <b>39</b> |
| 5.1      | Friction  | 39        |
| 5.2      | Setup (and suggestions for future improvements) | 40        |
| <b>6</b> | <b>Acknowledgements</b>                         | <b>43</b> |

## Introduction

Many people know ice is slippery, mostly by experience. Many know that ice is especially slippery when standing on it on two pieces of slightly curved steel. The slipperiness of ice is something that most of us accept without thinking about it. But why is ice so slippery? What makes it any different from other smooth surfaces, such as metal or glass? Nobody really knows.

Modern research in physics is advanced. It is surprising that such a seemingly simple thing as the friction of ice is not yet fully understood. There are several theories about it (which will be briefly explained in the next chapter), but there is not yet a single theory that is generally accepted. Possibly this is the case because the friction of ice is influenced by many things. One of the theories predicts that there is a thin lubricating water layer between ice and a sliding object, causing the low friction. This theory is the basis for the "skating project", of which this project is a part. During the skating project, a method is developed for measuring the water layer between the ice and a skate. In the current project, a setup is developed to continuously measure friction of ice during ice skating. In the future, these friction measurements are to be combined with the water layer measurements, that have already been performed previously, for a better understanding of the friction mechanism.

This thesis contains an overview of the setup, the results of the calibration of the setup, the results of the friction measurements and recommendations for future improvements of the setup.



## Previous work

In this chapter, previous work on both ice friction theory and ice friction measurements is discussed.

### 2.1 Theory

#### 2.1.1 Water layer

This project is based on the theory that the slipperiness of ice is caused by a water layer generated on the ice during skating. There are three hypotheses on how this water layer originates. The hypotheses are explained in more detail in the thesis of Jorinde van de Vis [1].

##### **Frictional heating**

Friction causes heating of the two objects sliding against each other. The amount of heat generated by friction is:

$$P = \mu \cdot F_n \cdot v$$

It was suggested to be the origin of a water layer between ice and a sliding object by Bowden and Hughes in 1939 [2].

##### **Pressure melting**

The phase diagram of water (figure 2.1) shows that, around its melting temperature, adding pressure could turn solid ice into liquid water. In 1859, Thomson [3] suggested that this could cause a water layer between ice and a sliding object.

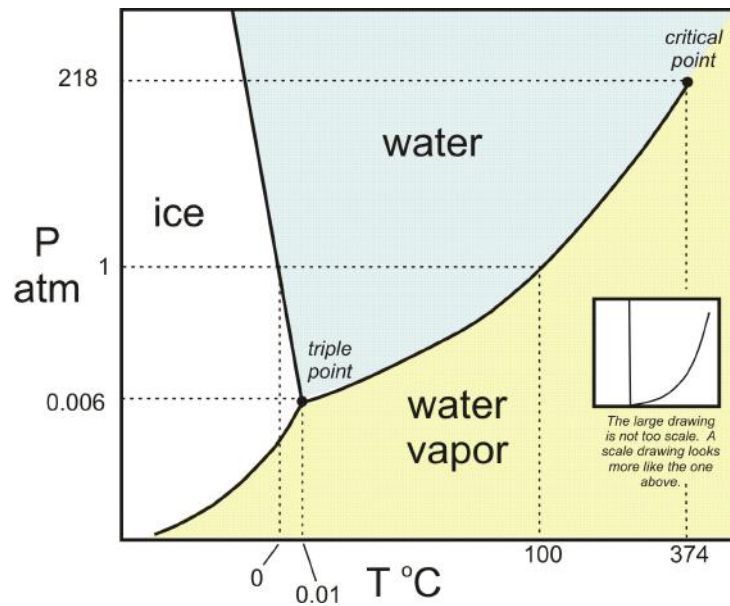


**Figure 2.1:** The phase diagram of water, not to scale. Around the melting temperature, increasing pressure can turn solid ice into liquid water.

### Surface premelting

In 1859, Faraday proposed the theory that the surface of ice always has a layer of liquid water on it, because two ice cubes brought into contact froze together after some time. The phenomenon was only explained in 1972 by Lacmann and Stransky [4].

### 2.1.2 Other theories

#### Surface diffusion

A different explanation for the ice cubes freezing together was given by Kingery in 1960 [5] and is based on surface diffusion. It states that molecules on a surface move randomly, and diffuse much like molecules in water. Ice friction measurements were done by Bart Weber [6] to confirm this theory.

#### Plastic and elastic deformation

A recent additional ingredient was formulated by H. van Leeuwen [7]. He noted that plastically deforming ice during skating costs energy. The normal force on the ice, curvature of the skate and skating speed can influence

the rate at which plastic and elastic deformation occur, and thereby adds a speed dependent contribution to the friction between the ice and the skate.

## 2.2 Previous research

All images in this section are taken from Kietzig et al. [8]. In this paper, results of many studies have been combined and compared.

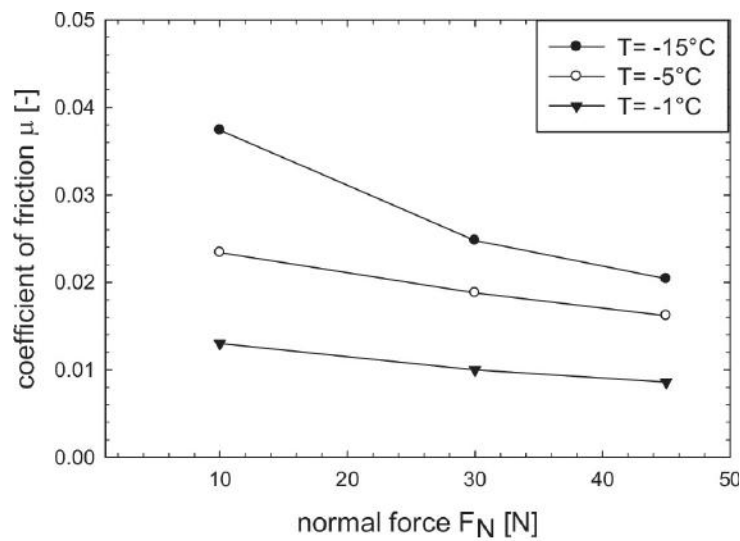
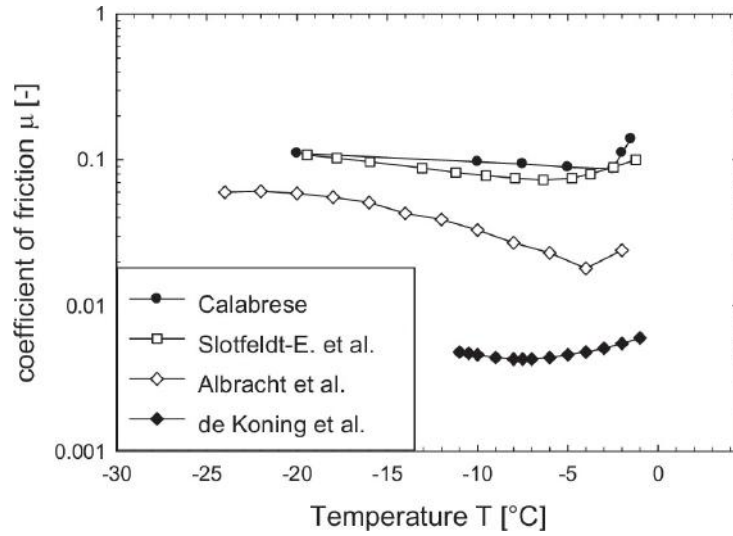


**Figure 2.2:** Friction coefficients as function of applied normal force and temperature ( $T$ ). Image from [8], data from Oksanen et al. [9]

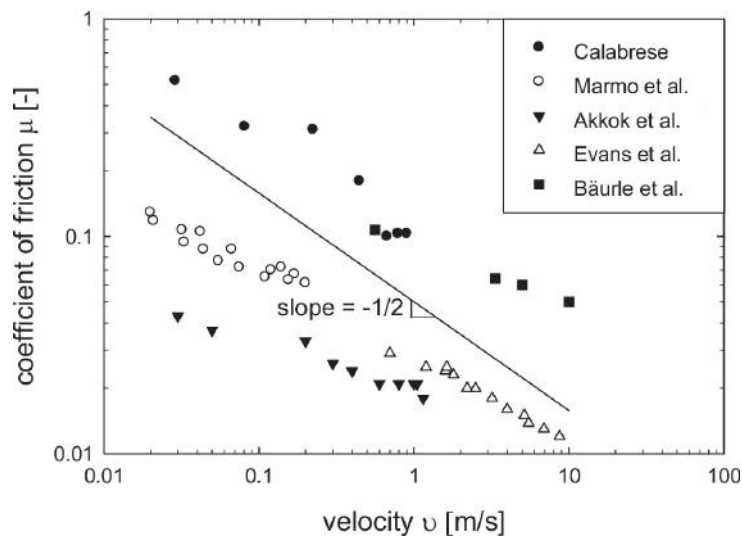
Figure 2.2 shows the friction coefficients of ice as function of normal force and temperature as measured by [9]. The graph shows that friction coefficients decrease with increasing temperature between  $-15^\circ\text{C}$  and  $-1^\circ\text{C}$ , and decrease with increasing normal force. The friction coefficients in this study range from 0.01 to 0.04.

Figure 2.3 shows the friction coefficients as function of temperature, from four different studies. The results from de Koning et al. [13] are from an experiment performed with an actual ice skater. All results show a decrease in friction coefficient with increasing temperature, up until a temperature of somewhere between  $-7^\circ\text{C}$  and  $-4^\circ\text{C}$ . The friction coefficients in these studies range from about 0.004 to 0.2.

Figure 2.4 shows the friction coefficients of ice as function of velocity. These results show that the friction coefficient of ice decreases with increasing velocity, for speeds up to 10 m/s. The friction coefficients in these studies range from 0.01 to 0.5.



**Figure 2.3:** Friction coefficients as function of ice temperature. Image from [8], data from Calabrese et al. [10], Slotfeldt-E. et al. [11], Albracht et al. [12], De Koning et al. [13]



**Figure 2.4:** Friction coefficients as function of velocity. Image from [8], data from Calabrese et al. [10], Marmo et al. [14], Akkok et al. [15], Evans et al. [16], Bäurle et al. [17]

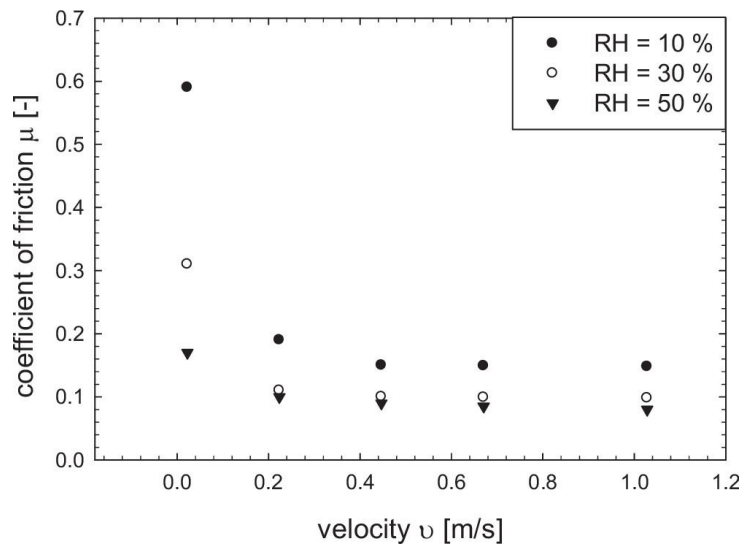


**Figure 2.5:** Friction coefficients as function of velocity and relative humidity (RH). Image from [8], data from Calabrese et al. [10]

Figure 2.5 shows the friction coefficients as function of velocity and relative humidity. This graph shows that the friction coefficient of ice decreases with increasing velocity, as in figure 2.4. It also shows that, at low velocities, the relative humidity can change the friction coefficient of ice up to a factor of 4.

From all of these results, it is clear that the friction coefficient of ice depends on many factors, and can vary over a few orders of magnitude.



# Chapter 3

## Setup

Over the course of the skating project, the setup has become increasingly complex. In this chapter, an overview of the setup is given, and parts of the setup relevant to the current project are shown in more detail.

### 3.1 General

In this section, an overview of the main setup is shown. Figure 3.1 shows the main setup components, but not the auxiliary equipment, such as the cooling control systems and measurement systems. The whole setup as shown in figure 3.1 is enclosed in an insulating box during measurements.

#### 3.1.1 The ice

In these experiments, a 150 $\mu$ m thick ice layer is used. Because the friction measurements are to be combined with the water layer measurements, the friction measurements should work with an ice layer thin enough for water layer measurements[18].

A smooth layer of ice is made by pressing a piece of glass coated in Rain-X (water-repellent coating) on a thin layer of water. The coating is necessary for easy removal of the glass after the water has frozen. The thickness of the ice layer is controlled by two spacers on the sides of the skate track. The surface below the water is then cooled until the water freezes and reaches the desired temperature.

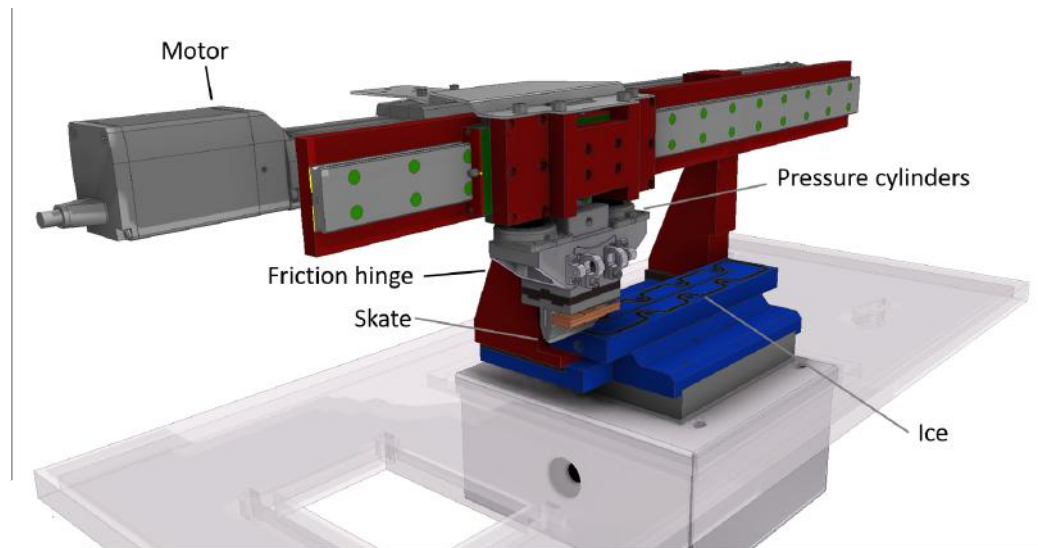


**Figure 3.1:** Overview of the main part of the setup. The skate, motor and friction measurement hinge are shown. The red part is the rail over which the skate moves. The blue part is a vacuum holder, on which any flat object can be placed. The blue part can be cooled so an ice layer can be grown on top.

### Observations on ice growth

It was found that for temperatures above  $-10^{\circ}\text{C}$ , the ice could not always handle high normal forces (above 200N). There were no problems when the ice temperature was below  $-20^{\circ}\text{C}$ .

The water was supercooled several times and froze instantly after tapping the glass. This may have influenced the structure of the ice and therefore caused it to break more easily, but it has not happened often enough to be verified.

### 3.1.2 The skate

The skate used in the setup is a 5cm long piece cut out of a real skate with a radius of curvature of 22m.

### 3.1.3 Water layer measurements setup

During this project, no water layer measurements were done. A full description of the most recent setup for water layer measurements can be found in the thesis of Max Snijders [18].

## 3.2 Setup: environmental & skating controls

This section is about the skate motion and control of the experimental environment. Many of the control systems have been improved since the previous part of the project. The two main improvements are:

1. lower temperatures (down to  $-30^{\circ}\text{C}$ ) can be reached and temperature control has been improved.
2. higher vertical normal forces on the skate can be applied to make the skating process more realistic.

Several control systems are not mentioned in this thesis, because they were not used during the project. This includes the equipment used for water layer measurements.

### 3.2.1 Temperature controls

The ice, skate and air are cooled by Peltier elements. All Peltier elements are controlled by feedback systems, which measure the temperature of the setup via thermocouples. The air temperature can be controlled by controlling  $\text{N}_2$  flow from a  $\text{LN}_2$  container to the setup. This has to be done manually.

#### Insulation

The setup is contained in a box. Before the start of this project, a new box was made. The previous box covering the setup was made of a single layer of plastic, without any additional insulation. It was too small for the motor rail, so the ends came out through large holes, allowing cold air to escape.

The new box (as seen in figure 3.2) is large enough to contain the entire setup as shown in figure 3.1. All cables and tubes exit the box through small holes in the bottom. The box is made of two layers of transparent plastic with an insulating layer of aerogel coated in reflecting foil in between. There is a single window in the box which has no insulating layer, and two holes that can be opened or closed.



**Figure 3.2:** The new insulating box around the setup. The entire box is made of a double layer of plastic with insulating aerogel coated in reflecting foil in between. There is a single window on the top, and two holes that can be opened on the front (the left hole is closed, the right hole is open).

### **Peltier cooling**

In the old setup, the skate and ice were cooled with Peltier elements by changing the voltage on the Peltier elements manually. In the new setup, the skate is cooled with twice as many Peltier elements, and air cooling with Peltier elements is added. Controllers are added for all Peltier elements, so the temperatures can be monitored and kept stable automatically.

### **Chiller**

The temperature difference of the hot and cold sides of the Peltier elements is about  $30^{\circ}\text{C}$ . In order to cool down the setup to temperatures around  $-30^{\circ}\text{C}$ , air cooling of the Peltier elements with a fan has been replaced by cooling with liquid coolant. The chiller is a device that decreases the temperature of the coolant to about  $-10^{\circ}\text{C}$ . It is then transported to the setup through tubes.

### **N<sub>2</sub> cooling**

During the project it was found that the Peltier cooling for the air was not sufficient to reach low temperatures. The Peltier elements increased the temperature of the coolant to such an extent that the chiller could not keep up. Therefore a LN<sub>2</sub> container was connected to the setup, blowing gaseous N<sub>2</sub> into the box. The temperature of this N<sub>2</sub> at the entrance of the

box could go down to at least  $-90^{\circ}\text{C}$ . An additional function of the  $\text{N}_2$  was lowering the relative humidity of the air inside the box.

### Temperatures

Many changes have been made to the cooling system, which, together with a new insulating box, make much lower temperatures possible. With the old system, minimum temperatures of  $-10^{\circ}\text{C}$  for the ice and  $-5^{\circ}\text{C}$  for the skate could be reached. With the new cooling system, the temperatures as given in table 4.1 can be reached.

Besides  $\text{N}_2$  cooling, Peltier elements can be used for air cooling. This is

**Table 3.1:** Temperatures in setup achieved with the new cooling system.

| Component | Temperature            | Method               |
|-----------|------------------------|----------------------|
| Skate     | $-22^{\circ}\text{C}$  | Peltier cooling      |
| Ice       | $<-30^{\circ}\text{C}$ | Peltier cooling      |
| Air       | $<-25^{\circ}\text{C}$ | $\text{N}_2$ cooling |

however much less efficient, and demands too much of the chiller. The downside of cooling with  $\text{N}_2$  only is that the humidity of the air is directly linked to the  $\text{N}_2$  flow, and thus to the temperature. As both the humidity and the temperature may affect the friction of the ice, these two variables should not be linked and changed together.

However, if  $\text{N}_2$  cooling is combined with Peltier cooling, the humidity will also depend on whether the Peltier element is active. The air cooled by the Peltier element comes from outside the box and contains much more water than the air inside the box. This adds uncertainty to the measurement.

### 3.2.2 Motor

The skate is moved by an IAI ROBO Cylinder (type RCP4-SA5C-I-42P). It accelerates up to  $1g$  and can reach speeds up to  $1400\text{mm/s}$ . When measuring motor speeds with the motor controller program, it was found that only speeds that are a multiple of  $25\text{mm/s}$  could be achieved, even when setting a speed that was not a multiple of  $25\text{mm/s}$ . It is unclear whether this is what actually happens to the speed, or if this is an erroneous result from the measurement program, as the controller program without any warning accepts speeds that are not a multiple of  $25\text{mm/s}$ .

### 3.2.3 Vertical force

The vertical force on the skate is applied by two cylinders that move under an applied air pressure. The air pressure can vary between 0 and 6 bar, with an accuracy of about 0.1 bar. A small spring holds the skate up, so it does not touch the surface when no air pressure is applied.

The skate is now mounted on a separate rail instead of directly on the driving motor, so it can handle the higher normal forces (the new rail is depicted in figure 3.1).

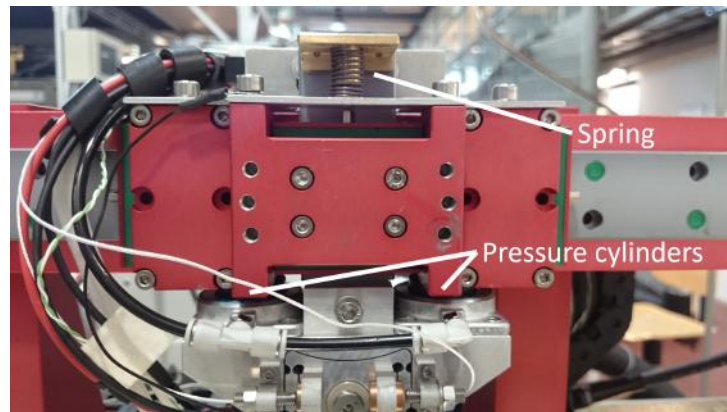


**Figure 3.3:** The system applying the vertical force. There is a spring holding the skate up, and two pressure cylinders pushing the skate down.

#### Calibration

The vertical force on the skate corresponding to a certain applied air pressure is determined in three different ways.

##### Method 1: Calculation

The skate is held up by a small spring. The force needed to push the skate down to the surface is measured to be  $20 \pm 5\text{N}$ . The large error is caused by the friction between the spring and the holder, making it hard to determine the exact force needed. The skate is pushed down by two cylinders with a diameter of 25mm, with a total area of  $9.81\text{cm}^2$ . This corresponds to a force of 98.1N per bar of pressure. This results in a conversion formula from pressure to force:

$$F_n = -20\text{N} + 98.1\text{N}/\text{bar} \quad (3.1)$$

**Method 2: At what pressure does the skate touch the surface?**

The second method links the pressure and force needed to push the skate down to the surface. This is the least accurate method due to the large error in the measured force necessary for the skate to touch the surface below. The pressure needed to push the skate down was 0.7 bar. The force per bar would then be 28.6N/bar. This results in the equation:

$$F_n = -20N + 28.6N/bar \quad (3.2)$$

This method can also be used to calculate the force of the spring, by assuming that the calculated 98.1N per bar is correct. The force of the spring is then calculated to be 69N, which is very different from the measured force. The equation then becomes:

$$F_n = -69N + 98.1N/bar \quad (3.3)$$

**Method 3: Direct measurement**

The results of the previous two methods do not match. This means that either the measured force of the spring is wrong, the force calculated from the cylinder diameter is wrong, or the pressure to push the skate on the surface was not 0.7 bar. A direct measurement of the force on the skate is possible by pushing the skate on a weighing scale and reading off the weight for a certain pressure. The results of two of these measurements are shown in figure 3.4. This graph shows that the pressure needed to push the skate down is about 0.6 to 0.7 bar. The slope between the two measurements varies by 30%, possibly because of the different positions of the skate on the scale. This shows that even direct measurement of the force on the skate is not very accurate. The equation for the normal force resulting from the direct measurement on the center of the scale is:

$$F_n = -39N + 65N/bar \quad (3.4)$$

and on the edge of the scale:

$$F_n = -30N + 50N/bar \quad (3.5)$$

**Used calibration**

Because the results of the different calibrations vary by up to a factor of 2, the normal force on the skate can not be determined accurately. In this

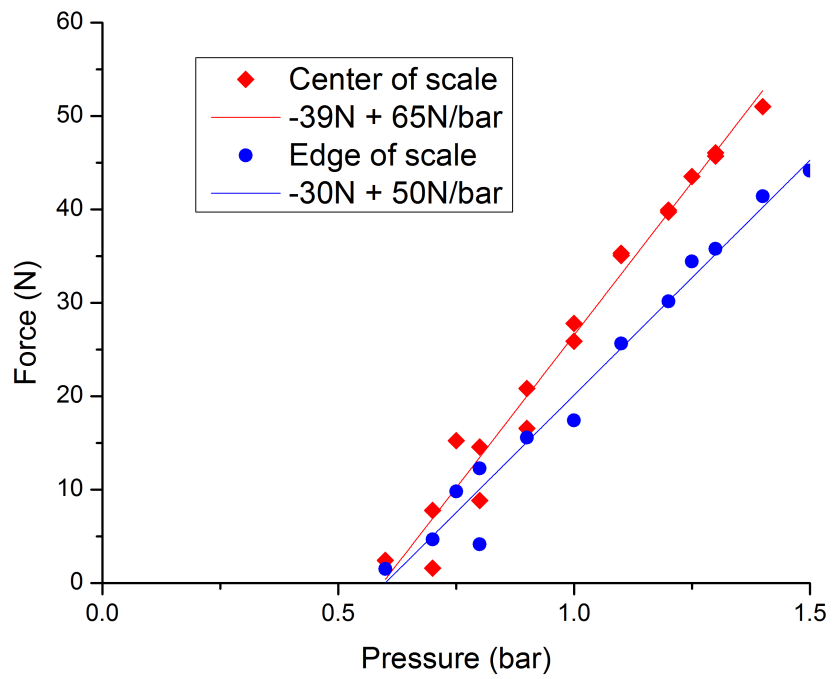


**Figure 3.4:** Measured vertical force for different pressures.

thesis, the results of the direct measurement on the center of the scale will be used to convert the pressure to a normal force, because this result is in between the other results, and because it is a direct measurement and thus most reliable. Both the pressure and the normal force (calculated using equation 3.4) will be shown in the results chapter.

### 3.3 Friction measurements setup

With the old setup, the friction between the skate and the ice could not be measured. A system has been added with which the friction can be measured continuously, for simultaneous water layer and friction measurements. The system is explained in this section. It has not been tested before, and was tested and calibrated during this project.

#### 3.3.1 Hinge

A special hinge was designed by the Merlijn Camp and Gert Koning of the FMD to be flexible in the horizontal direction and very rigid in the vertical direction. It was designed this way because it has to measure relatively small friction (horizontal) forces under a large vertical normal force. The hinge is shown in figure 3.5, with sensor holders mounted on both sides. The figure also shows an exaggerated view of how the hinge deforms under a vertical force 25 times larger than the horizontal force.

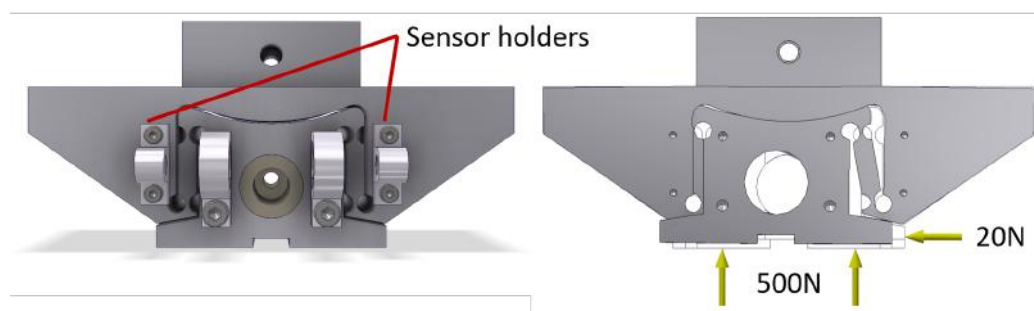


**Figure 3.5:** Left: the hinge with sensor holders. Right: an exaggerated view of how the hinge deforms under a vertical force of 500N and a horizontal force of 20N.

### First version of hinge

The first version of the hinge had unintended weak spots at the top, which could have caused it to rotate. Rotation of the hinge cannot be measured. This creates uncertainties in the measurement. Furthermore, rotations in the hinge can change the contact point of the skate to the ice, possibly changing the friction. Therefore a new hinge without the weak spots was designed during the project and used for measurements.

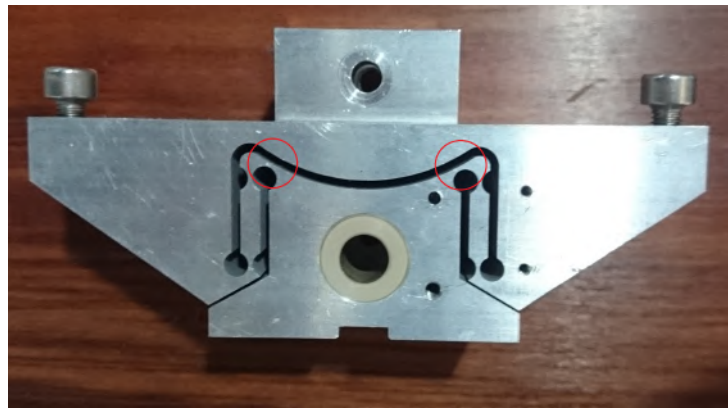


*Figure 3.6: The old hinge, with weak spots at the top, indicated by the red circles.*

### 3.3.2 Sensors

In the setup, two M-DVRT sensors are used. The sensors measure the distance to a piece of copper, with a resolution of 300nm. The sensors are mounted on the outer part of the hinge (figure 3.5), and the copper pieces on the inner part. The sensors are placed in the opposite direction of each other. If a horizontal force is applied, such as depicted in figure 3.5, the inner part of the hinge moves to the left, decreasing the distance between the left sensor and the copper, increasing the sensor's output voltage. On the other hand, it increases the distance between the right sensor and the copper, and thus decreases the output voltage.

#### Why two sensors?

If the sensors are calibrated correctly and the hinge works the way it should, the changes in output voltage should be perfectly antisymmetric. Both sensors would give the same information and we would need only one sensor for the measurement. The reason there are two sensors, is because

the hinge is not perfect and also deforms when a vertical force is applied. There are many ways in which it can deform. The inner part can be pushed up, increasing the distance of both sensors to their copper piece. It can also be compressed in the vertical direction and thus stretched in the horizontal direction, decreasing the distance between the sensors and the copper. The important thing about these deformations is that they should all be symmetric, as the hinge is symmetric. With two sensors, the symmetric changes in output voltage are thus due to the vertical force, while the antisymmetric changes are due to the horizontal force. With only one sensor, there is no way to know how much the vertical force contributes to the change in voltage. Figure 3.7 shows how the contribution of the horizontal force to the change in voltage can be filtered out. When adding the signals of the two sensors, the contribution of the vertical force is left. When subtracting the two, only the contribution of the horizontal force is left.

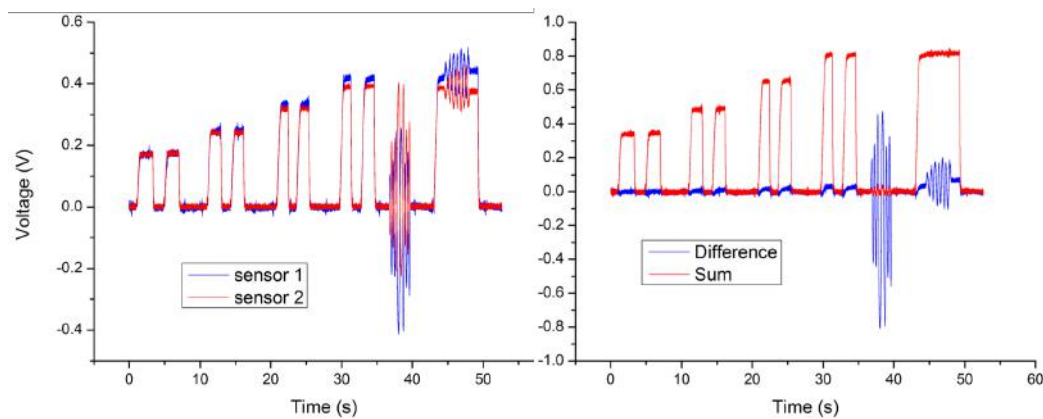


**Figure 3.7:** Left: the signal of the two sensors during a test measurement. First, the pressure was turned on and off several times, causing the peaks in the signal. Then, without the pressure on, the hinge was pulled back and forth horizontally. Then the pressure was turned on and a horizontal force was applied to the skate. Right: the sum and difference of the two signals. The sum shows only the contribution of the vertical force, and the difference shows only the contribution of the horizontal force.

### Effect of vertical force & comparing the sensors

In figure 3.8 it can be seen that the voltage of the sensors increases with increasing pressure on the skate. However, the slope of the voltage is different for both sensors. This can have several explanations. One of the

explanations is that the hinge is not perfectly symmetric and deforms asymmetrically. Another explanation is that the two sensors do not have the same sensitivity. Their sensitivity depends on the equilibrium voltage, and the sensitivity of both sensors can be tuned so they are as close to each other as possible. Figure 3.9 shows this effect.

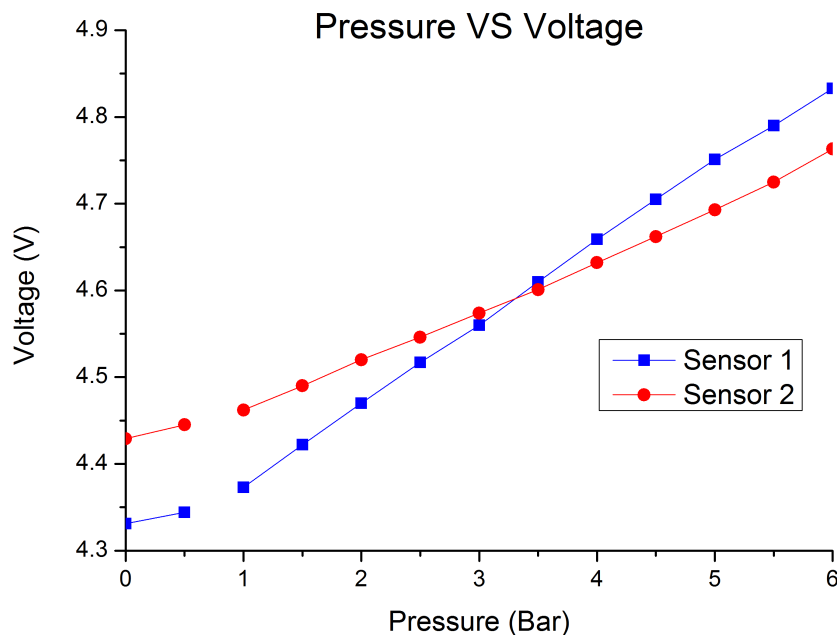


**Figure 3.8:** The voltage of the sensors as function of the applied pressure. The slope is different below 1 bar, because the skate does not yet touch the surface at such a low pressure. The small slope below 1 bar may be caused by the pressure cylinders pushing on the hinge and deforming it.

### 3.3.3 Calibration of the hinge

In general, the calibration of the hinge is done by hanging varying masses of 0 to 2 kg on a string, which is connected to the skate via a pulley to exert a horizontal force on the skate. The output voltages of the two sensors are measured using a DAQ card.

For measurements with a normal force on the skate, the pressure can either be applied after the horizontal force, or before. The pressure on the

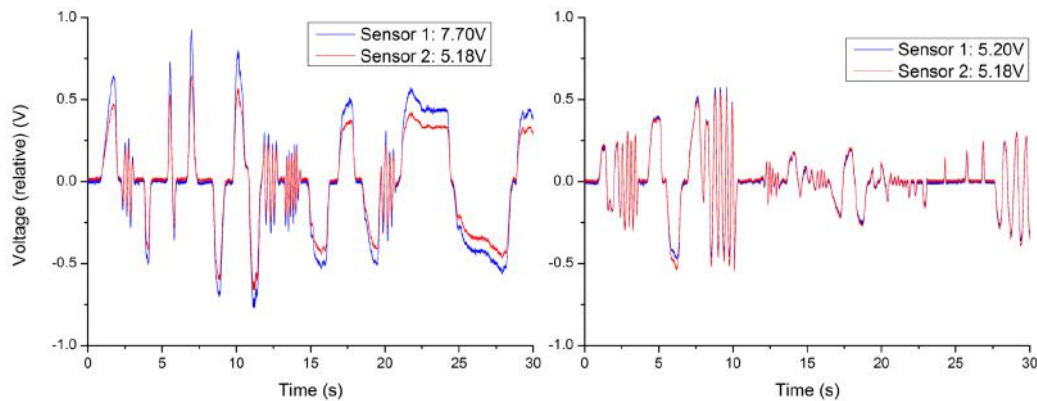


**Figure 3.9:** Left: the signal of the two sensors when the equilibrium voltages are not equal. The sensitivity of the sensors differs. Right: the signals when the equilibrium voltages are equal. The sensitivity of the sensors is very similar in this situation.

skate causes a large friction force between the skate and the surface below, which can prevent the skate from moving when a horizontal force is applied, preventing the hinge from deforming horizontally. Thus, in our measurements we first apply the horizontal force and then the pressure. The measurement is done with pressures of 0 bar, 3 bar (156N) and 5 bar (286N).

The results of the calibration are shown in figure 3.10. The calibrations for both 0 and 3 bar are linear, and the linear fits through all of the data sets (for both sensors and both directions of the force) are quite similar for 0 and 3 bar. Note however that the slopes of the fits vary, especially between positive and negative forces. It is not clear why the slope varies, it is possible that the hinge is not exactly symmetric and deforms more easily in one direction than the other. It is also possible that the nonlinear sensitivity of the sensors causes the slope to be different for increased and decreased distance to the copper. For both sensors, and both 0 and 3 bar, the slope is 0.003 larger when the distance is decreased, than when the distance is increased.

The results for 5 bar are not as linear, and therefore the fit is not as good as the fit for 0 and 3 bar. The slopes of the fits are however quite similar to the slopes for 0 and 3 bar. Therefore, in this thesis, the calibration for 3 bar is used for all measurements. Calibration for 3 bar is a compromise between

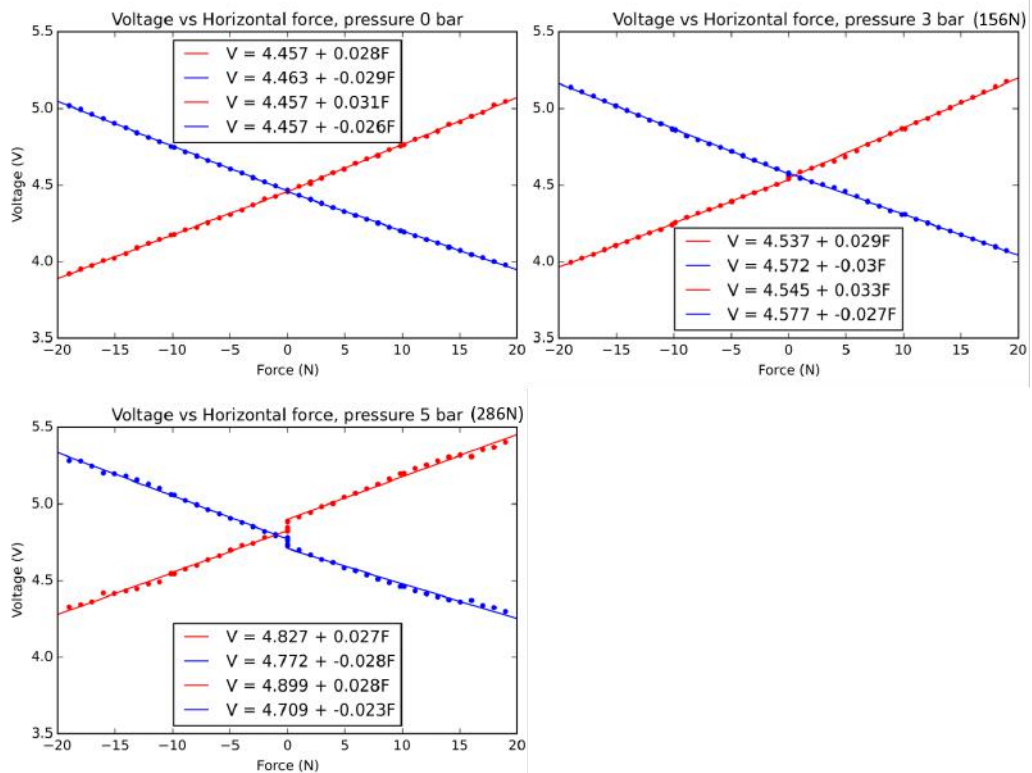


**Figure 3.10:** The calibration of the hinge for 3 different applied pressures. The formulas for the linear fit of each set of data for both sensors and both directions of the force are shown in the graphs. The calibration for 0 and 3 bar are both linear and have similar slopes. The calibration for 5 bar is not as linear and therefore the fit has a different slope.

---

the reliable measurement with no pressure (and no friction force), and the realistic pressure of 5 bar used in many measurements.

### 3.3.4 Friction measurements methods

Friction between skate and ice is measured using the sensors described in this chapter. The friction force can be directly related to the sensor output voltage by calibration. Before the measurement starts, the skate is set to alternately skate back and forth at two different velocities. The slow speed is always 30mm/s and the fast speed is either 100mm/s or 200mm/s. The friction measurements are done under varying circumstances. Varied parameters include vertical force on the skate, skating speed and air, skate and ice temperatures.



## Results and discussion

In this chapter, results of the friction measurements are shown and discussed. The general recipe for friction measurements is: skate back and forth at two different velocities. More specifically: skate forwards fast, skate backwards fast, skate forwards slowly, skate backwards slowly. "fast" was always either 100mm/s or 200 mm/s, and "slow" was always 30mm/s. All results shown in this thesis were obtained during a single day, on the same ice layer, except for the ice profile measurement in section 4.3. Parameters of all of the measurements are included in appendix A.

The friction force as function of time is expected to look like figure 4.1, assuming the friction force is constant during skating.

The data can then be divided into 4 categories: slow forward (sf), slow backward (sb), fast forward (ff) and fast backward (fb). Slicing the data and plotting all runs of each category over each other, changes in the friction can be seen. In many of the figures in this chapter, a single category was chosen (usually slow forward, sf) and compared between different measurements.

### 4.1 Friction on teflon

In order to test the setup, friction measurements have been done on other surfaces than ice. Figure 4.2 shows the friction of a metal strip on teflon and the friction of the skate on ice. The data has been cut to show only a single slow forward and slow backward run (30mm/s). Since the friction coefficient of teflon is higher than the friction coefficient of ice, a lower vertical force is used in the teflon measurements. Higher forces on teflon

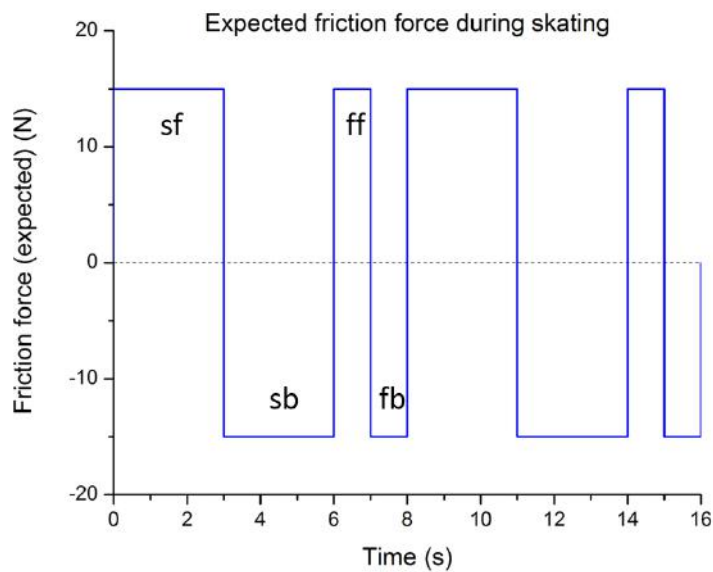


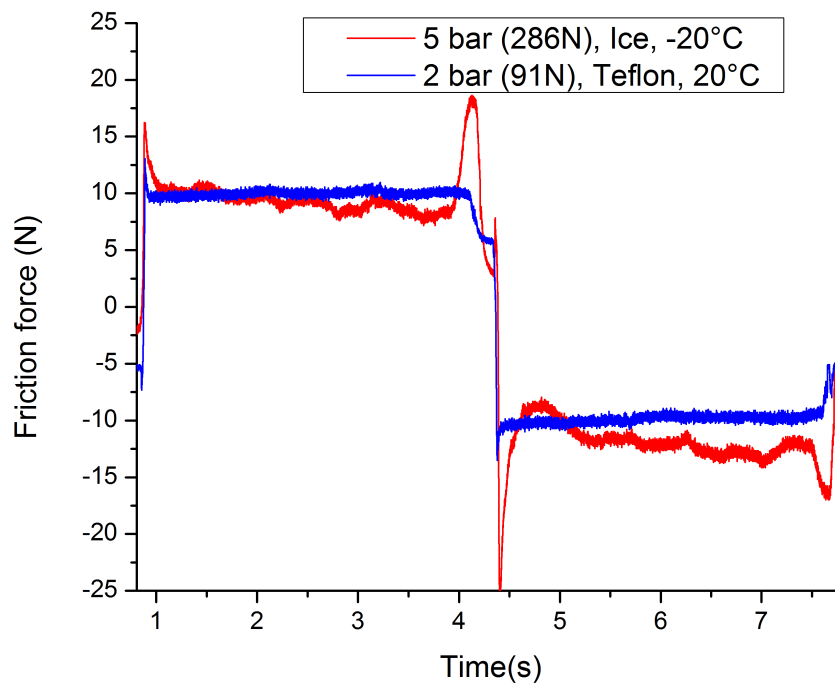
**Figure 4.1:** An example of what the friction as a function of time should look like. In the graph, the four categories are shown: slow forward (*sf*), slow backward (*sb*), fast forward (*ff*), fast backward (*fb*).

will result in friction forces too high for the hinge, and lower forces on ice will result in data with a low signal to noise ratio. The friction of teflon is very regular and looks much like the example. The only difference is a peak at the start of a run, and a dip at the end. This is just the force on the hinge caused by the acceleration and deceleration of the skate. The measured friction coefficient of teflon is 0.11. This is within the range of 0.05-0.2 found in literature[19]. The friction on ice does not look as regular. These irregularities will be investigated in the next sections.

## 4.2 Time dependence

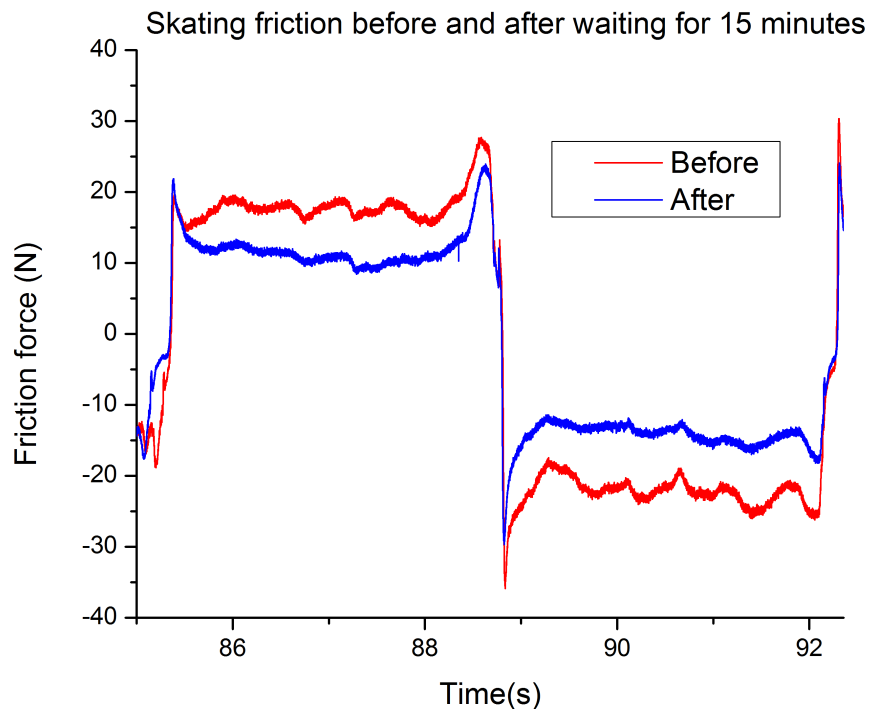
The shape of the friction as a function of time was studied to find out whether it changes during skating, or after leaving the ice alone for a while. When the ice is left alone, it could either grow or evaporate (depending on the humidity of the air), changing the shape of its surface.

Figure 4.3 shows the friction of the skate and the ice just before and just after a break of 15 minutes. The "before" run had been skating for a few minutes, directly after a few other measurements. Then, the ice was left for 15 minutes before starting to skate again. The "after" data shows one



**Figure 4.2:** The friction force during skating on ice and teflon at 30mm/s compared. The friction on teflon is very regular, but the friction on ice shows bumps.

of the first runs of the skate over the ice. Again, the data has been cut to show only a single slow forward and slow backward run. The most notable change is the decrease in friction force. The shape of the data has not changed much.



**Figure 4.3:** The friction force during a slow forward and slow backward run, before and after waiting for 15 minutes. There is a decrease in friction force, but the shape of the data does not change much.

Figure 4.4 shows all forward slow runs of three different measurements. Within the same measurement, the friction changes. Often the friction increased during a measurement, but this was not always the case. Between different measurements (with time and other measurements in between), there are large differences, up to a factor of two, in friction force, even though the temperatures, normal force and used skating speeds are kept constant. The similarity in shape between the three sets of data is striking.

The changes in friction may have been caused by a change in the ice surface, but it is also likely that they were caused by something else, possibly a changing air temperature (it was not stable) or changing humidity.

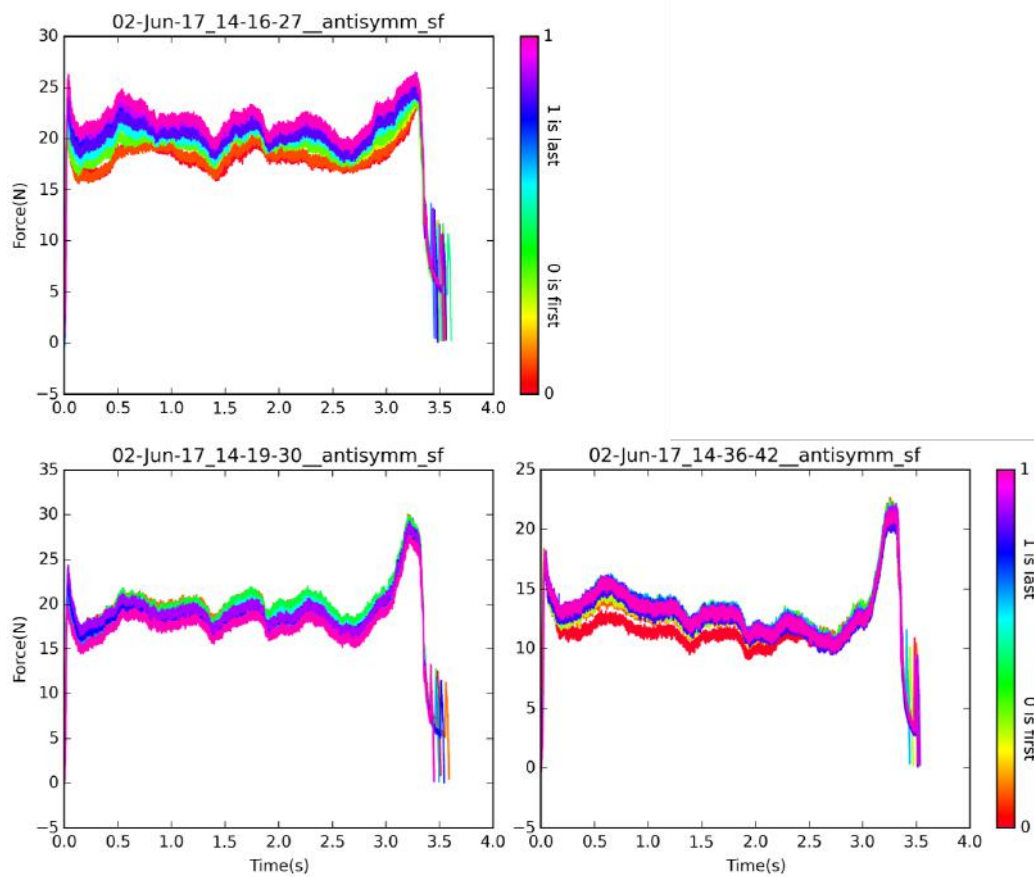


**Figure 4.4:** The friction force during the slow forward runs of three measurements under the same environmental conditions, at different times. There are large variations in the friction force, but the shape of the data does not change much.

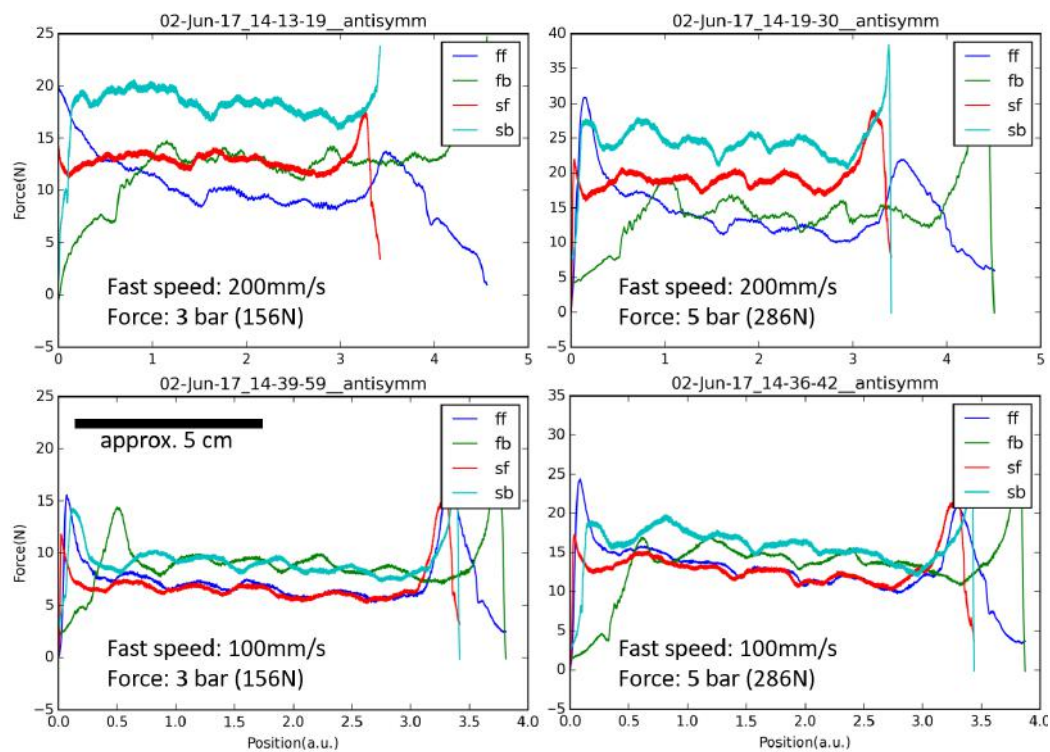
### 4.3 Space dependence

This section continues to focus on the shape of the data. In figure 4.5, data of all four categories (combinations of fast, slow, forwards and backwards) have been averaged per category. All data of backward runs have been flipped in time to match the forward runs in space, and fast runs have been stretched to match the slow runs. This results in the data plotted as function of approximate position. The position is approximate because the skate accelerates, decelerates and waits for some time between the runs. Therefore, position is not a linear function of time. This effect is stronger for measurements at higher speeds, because the accelerating and waiting times are relatively longer. This causes shifts between the data of different categories. However, when we want to look at similarities between forward and backward runs, we can look at fast and slow speeds separately. We are also mostly interested in the region where the skate is skating at a constant speed, because the acceleration and waiting times of the motor differed between runs. Especially in the slow runs, where the effects of the acceleration and waiting are less, the similarities between forward (red in the graphs) and backward (light blue in the graphs) runs are striking.

### 4.4 Height profile measurement after skating

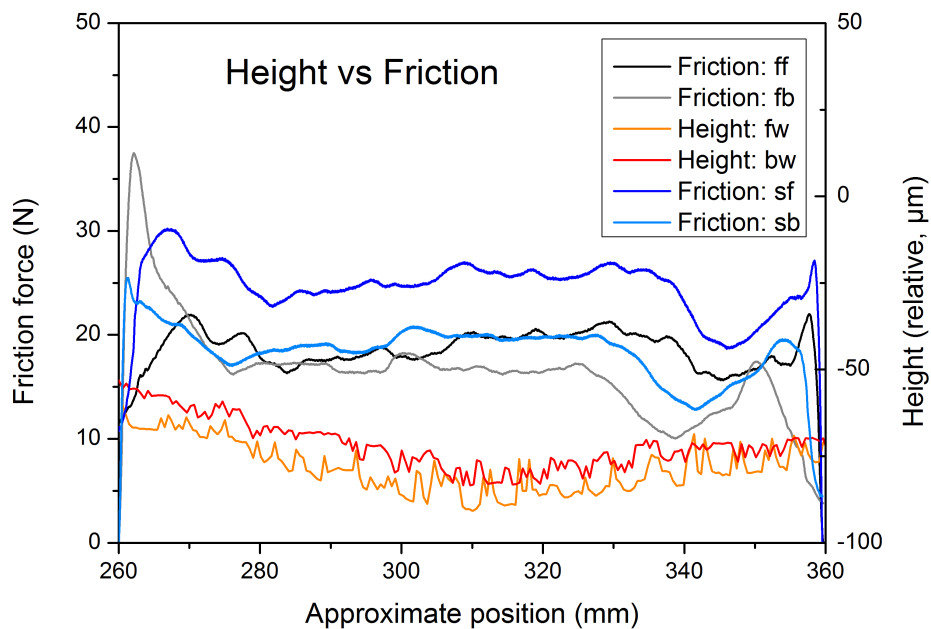
In all friction results in the previous sections, clear features can be seen in the friction as a function of time, even after averaging all runs. In figure 4.5, it becomes clear that these features are very similar in space for all runs, including different speeds and skating directions. The shape did however change a little over time, and was completely different when measuring on a different ice layer (figure 4.5 and 4.6 show measurements on different ice layers). This strongly suggests that the features visible in the friction are caused by the shape of the surface of the ice. Therefore an ice height profile measurement was done after a friction measurement, using a dial gauge[20]. The dial gauge is mounted on the skate holder and moved slowly over the ice, measuring height differences. It can be seen that the shape of the data is different from the shape of other friction data shown in this chapter.

Figure 4.6 shows all averaged runs of the friction measurement, and the height measurement that was done immediately after. It must be noted that the position for the friction is approximate, and it is possible the graph has to be shifted or even stretched. Even then, no clear similarities be-



**Figure 4.5:** The friction forces of 4 different measurements, averaged per category and plotted as function of approximate position. The shape of the data is very similar for all four categories, indicating a dependence on the surface of the ice. There is no difference in friction between fast and slow runs, when the fast speed is 100mm/s. There is a difference in friction when the fast speed is 200mm/s. The slow speed is 30mm/s in all measurements.

tween the height of the ice and the friction of the skate and ice can be seen. It is possible, but unlikely, that the height profile measurement was done next to the skate track, instead of in the skate track. This was however checked very carefully. It is also possible that, due to the large radius of curvature of the skate and curved ice, the contact between the skate and the ice was not in the center of the skate, but somewhere else. This would make the friction force depend not exactly on the position of the skate, but on the position of the contact point, which is not known. For now, it is not yet clear what causes the bumps in the friction force.



**Figure 4.6:** Results of a friction measurements (blue and gray lines) compared to the results of a height profile measurement (orange and red lines). The shape of the friction measurement may need to be stretched or shifted to match the position of the height measurement. There is no clear similarity between the friction and height profile results.

## 4.5 Speed dependence

In figure 4.5, a slow speed of 30mm/s has been used, and both fast speeds of 100mm/s and 200mm/s. For fast speeds of 100mm/s, there is no dif-

ference in friction between the slow and fast runs. In fact, the lines of different speeds (red and dark blue, and green and light blue) overlap almost perfectly. But for the fast speed of 200 mm/s, the friction of the slow speed runs is noticeably higher than the friction of the fast speed runs. The latter is in agreement with the results of previous research (figures 2.4 and 2.5).

## 4.6 Temperature dependence

There are two sets of temperatures that were used during skating, as shown in table 4.1. In the results, only the ice temperatures will be mentioned.

**Table 4.1:** Two sets of temperatures used for friction measurements.

| Component | Cold temperature | Warm temperature |
|-----------|------------------|------------------|
| Skate     | -10°C            | -10°C            |
| Ice       | -20°C            | -10°C            |
| Air       | -10°C            | -8°C             |

During a single measurement, the ice temperature was increased from -17°C to -10°C in less than 5 minutes. Figure 4.7 shows the skating friction during this measurement. The many individual runs of the skate can not be seen, but the darker blue parts show the regions where the skate was skating at a constant velocity. During the measurement, the friction force decreases with increasing temperature.

Figure 4.8 shows a single slow forward and backward run of two different normal forces and temperatures. The measurements with the same normal force are shown in the same figure. The frictions of the measurements with the higher temperature are much lower than the frictions of the measurements with the higher temperature. The shape of the data does not depend on the temperature. Both results are in agreement with results of previous research, where it was found that friction force decreases with increasing temperature, up to about -5°C. The friction then starts increasing again (figure 2.3).

## 4.7 Coefficient of friction

To calculate the friction coefficients, the averaged friction data (as in figure 4.5) have been used to estimate the average friction coefficient over the whole run. There is a lot of uncertainty in these friction coefficients, due to

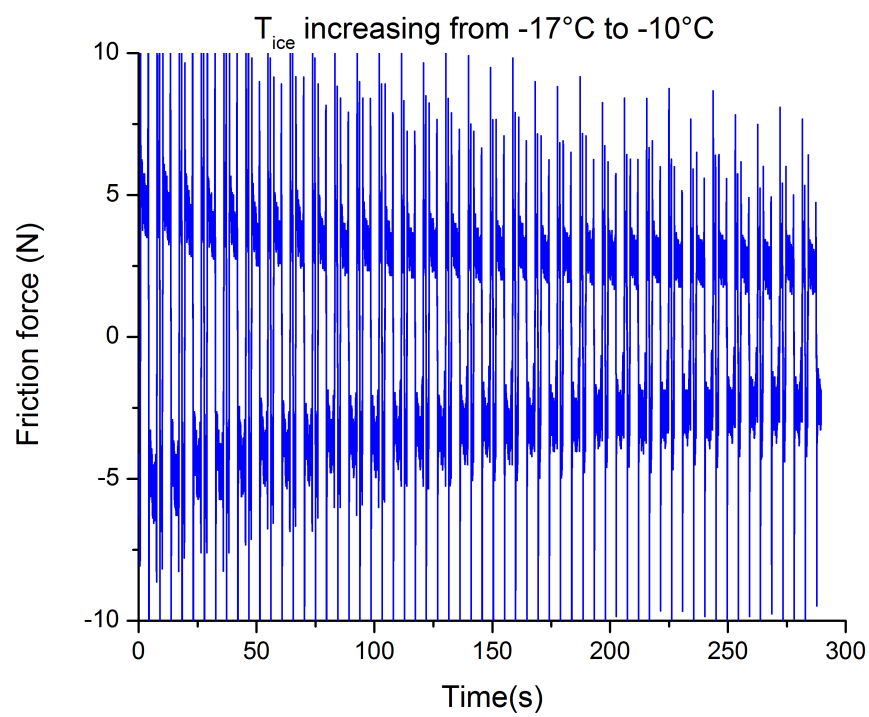


**Figure 4.7:** The friction force as function of time, with the temperature of the ice increasing from  $-17^{\circ}\text{C}$  to  $-10^{\circ}\text{C}$  during the measurement. The friction decreases with increasing temperature.

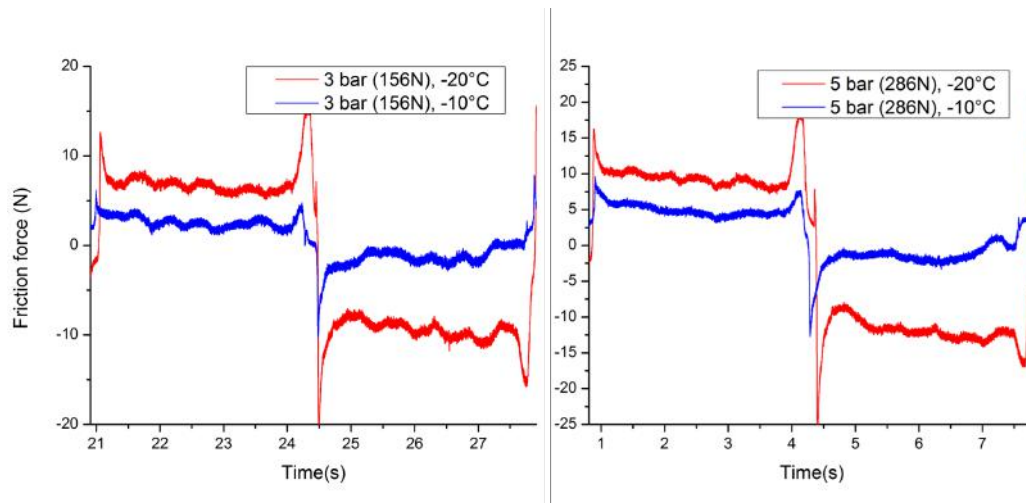


**Figure 4.8:** Left: the friction force of a single slow forward and backward run at 3 bar (156N) at ice temperatures of  $-10^{\circ}\text{C}$  and  $-20^{\circ}\text{C}$ . Right: the friction force at 5 bar (286N). The friction force is much lower at  $-10^{\circ}\text{C}$  than at  $-20^{\circ}\text{C}$ . The shape of the data does not depend on temperature.

an uncertainty in normal force (see section 3.2.3), uncertainties in voltage-force conversion (see section 3.3.3) and a varying friction force during the measurement.

Figure 4.9 shows the friction coefficients of all measurements done on June 2<sup>nd</sup>, except from the measurement where the temperature was increased. There are notable variations between results of measurements done under the same circumstances (in figure 4.9, all dots with the same colour on the same line are measurements with the same parameters). However, all friction coefficients measured at  $-10^{\circ}\text{C}$  are lower than all friction coefficients at  $-20^{\circ}\text{C}$ , hence there is a clear temperature dependence of the friction coefficient of ice. The speed dependence found in the previous sections can not be seen from this figure, because the variations in friction force between different measurements were larger than the differences in friction between fast and slow speeds. The variations are also too large to confirm any relation between friction and normal force. The friction coefficients vary between 0.006 and 0.016 for an ice temperature of  $-10^{\circ}\text{C}$  and between 0.04 and 0.1 for an ice temperature of  $-20^{\circ}\text{C}$ , which is in agreement with previous measurements reported in literature (section 2.2). A list of the measured friction coefficients can be found in appendix A.

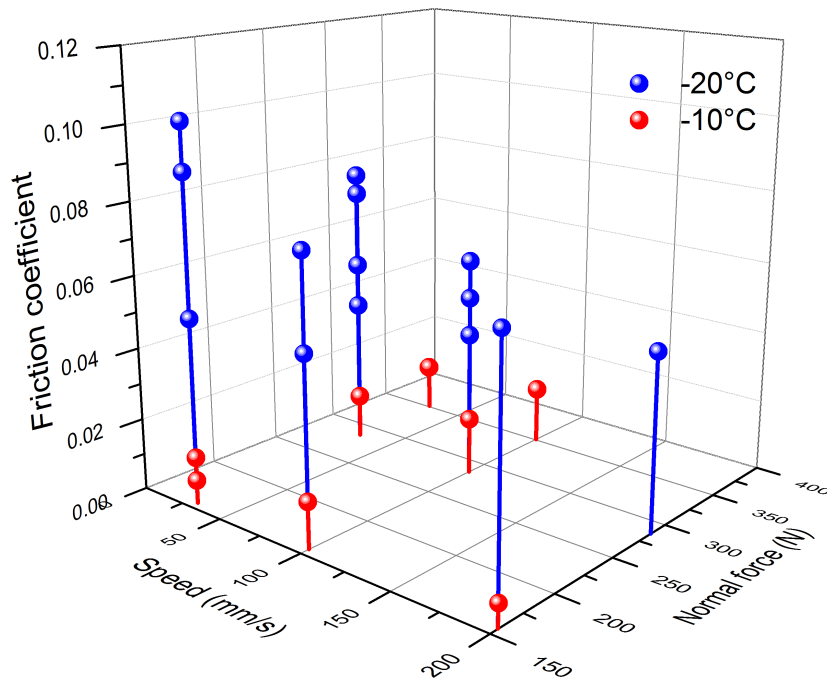


**Figure 4.9:** The friction coefficients for all measurements as function of skating speed, normal force and temperature. There are variations in friction force between measurements with the same parameters. However, a clear temperature dependence is observed. The friction coefficients vary between 0.006 (at  $-10^{\circ}\text{C}$ ) and 0.1 (at  $-20^{\circ}\text{C}$ ).

### 4.7.1 Normal force dependence

Figure 4.10 shows the data of all measurements at  $-20^{\circ}\text{C}$ , as function of normal force. Results of measurements with the same parameters have been averaged. The averaged friction coefficients for 3 bar (156N) are higher than the averaged friction coefficients for 5 bar (286N), suggesting a dependence on normal force. As the variation between friction coefficients of measurements with the same parameters (as seen in figure 4.9) is larger than the difference in friction coefficient between the two normal forces, this result has yet to be confirmed.

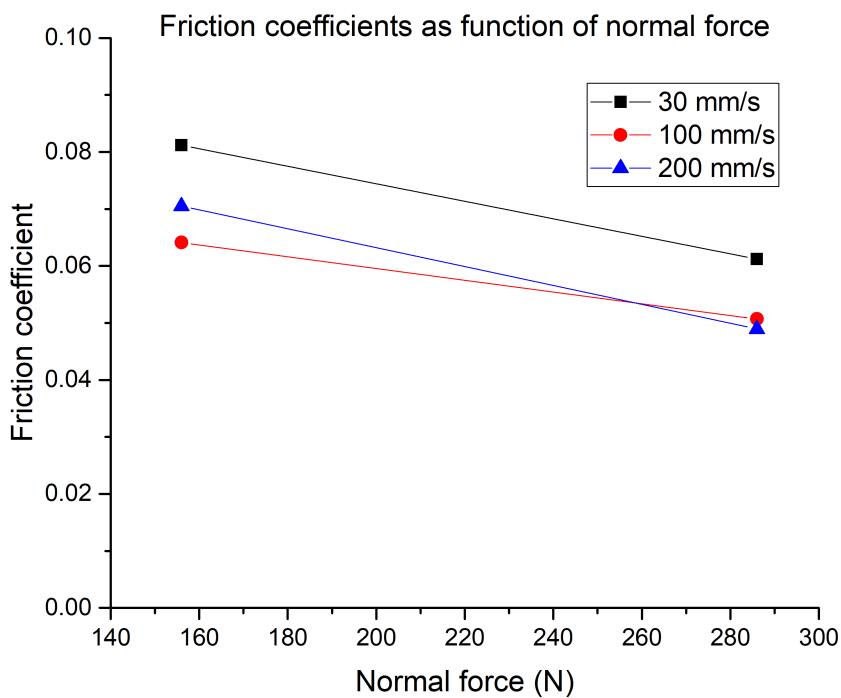


**Figure 4.10:** The friction coefficients for all measurements at  $-20^{\circ}\text{C}$  as function of normal force. The friction coefficients for each speed are averaged. The averaged friction coefficients for 3 bar (156N) are higher than the averaged friction coefficients for 5 bar (286N), indicating a dependence on normal force.

## 4.8 Humidity dependence?

The variations in friction forces between measurements could be attributed to the (possibly changing) humidity in the setup box. The air temperature was controlled by a flow of  $N_2$ , which can also change the humidity of the air. Figure 4.11 shows a previous result obtained by Calabrese et al. [10] (already shown in section 2.2). At slow speeds, the friction coefficient of ice depends on the humidity of the air, up to a factor of 4. As our measurements are all done at speeds below 0.2m/s, the humidity could influence the friction coefficient significantly, and have caused the variations as seen in figure 4.9.

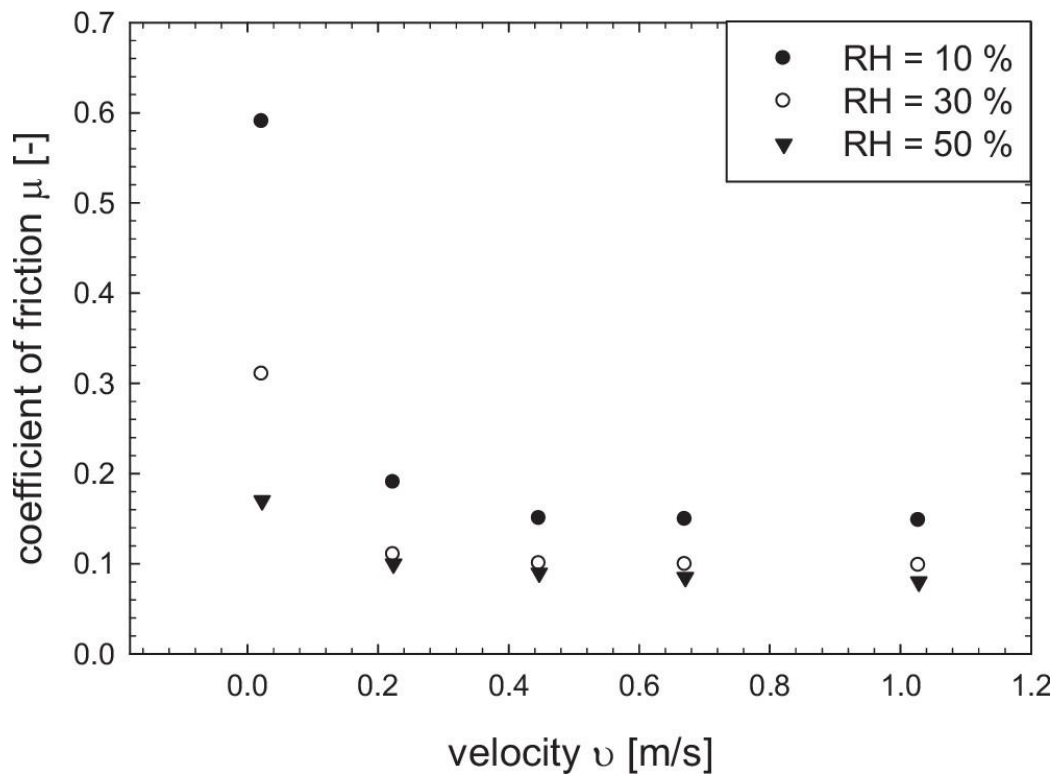


**Figure 4.11:** Friction coefficient of ice as function of velocity and relative humidity (RH) of the air. At speeds below 0.2m/s, the humidity of the air influences on the friction coefficient of the ice strongly, up to a factor of 4. The used ice temperature was  $-29^\circ C$  and the used normal force was 178N. Image taken from Kietzig et al.[8], data from Calabrese et al.[10].

## Conclusions & outlook

In this chapter, the conclusions drawn from the results of the friction measurements and setup testing are presented. It is also discussed how these conclusions affect the future direction of the project.

### 5.1 Friction

**In our setup, the friction varies during skating. It is not yet clear why.**

This could be studied in the future, as the variation in friction during a single run can tell us something about the ice friction mechanisms, especially combined with water layer measurements.

**A temperature dependence of the friction force during ice skating is verified.**

The friction of ice at  $-10^{\circ}\text{C}$  is lower than the friction of ice at  $-20^{\circ}\text{C}$  (figure 4.9). This is in agreement with results of previous research (figure 2.5).

**A speed dependence of the friction force during ice skating is suggested.**

The friction force is lower for higher speeds (figure 4.5 and figure 4.10). The variation in friction coefficients of measurements with the same conditions is larger than the variation in friction coefficients between the different speeds (figure 4.9), and there were only three different speeds used in measurements, so this result has to be verified.

**A normal force dependence of the friction force during ice skating is suggested.**

The averaged friction coefficients for 3 bar (156N) are higher than the averaged friction coefficients for 5 bar (286N) (figure 4.10), on ice of  $-20^{\circ}\text{C}$ . The variation in friction coefficients of measurements with the same conditions is larger than the variation in friction coefficients between the two normal forces (figure 4.9), and there were only two different normal forces used in the measurements, so this result has to be verified.

**The measured friction coefficients vary between 0.006 and 0.1. This is in agreement with previous research.**

This can be found in figures 2.2, 2.3, 2.4 and 2.5.

## **5.2 Setup (and suggestions for future improvements)**

**The setup for friction measurements works.**

This is shown by the test measurement on teflon, where the friction force as function of time has the expected shape and value (figure 4.2).

**The vertical normal force on the skate is uncertain, up to a factor of 2.**

For measuring the exact friction coefficients, the calibration of the normal force system has to be improved. A weighing scale or force sensor more suitable for the setup may be helpful. The actual air pressure in the setup could also be calibrated.

**The calibration of the hinge and sensors (sensor voltage to friction force conversion) is uncertain for large normal forces.**

The calibration measurement could be repeated with more different values of the normal force.

**Variation in friction force between measurements suggests changing conditions in the setup.**

This should be studied in the future, as it causes uncertainty in the measurement results. An air humidity sensor (and possibly a humidity control

system) would be a useful addition to the setup.



# Chapter 6

## Acknowledgements

During the project, there were many people around me who were always willing to help. First I want to thank Tjerk Oosterkamp, who supervised me during my project. I also want to thank Tom van der Reep, who is still very involved in the project, and was always available when I had questions. I also want to thank all the other people of the group, with whom I could discuss the results of my project during the weekly group meetings.

From the FMD, I want to thank Gert Koning for all help with the setup, for designing and making entirely new parts, or repairing broken ones. I want to thank Merlijn Camp for his contribution to the (re)design of the hinge. From the ELD, I want to thank Raymond Koehler, who helped me connect and fix all electronics of the setup.



# References

- [1] J. van de Vis, *Towards measuring the water layer thickness during ice skating*, Bachelor thesis, Leiden University, 2013.
- [2] F. Bowden and T. Hughes, *The mechanism of sliding on ice and snow*, in *Proceedings of the Royal Society of London A: Mathematical, Physical and Engineering Sciences*, volume 172, pages 280–298, The Royal Society, 1939.
- [3] J. Thomson, *On recent theories and experiments regarding ice at or near its melting-point*, *Proceedings of the Royal Society of London* **10**, 151 (1859).
- [4] R. Lacmann and I. Stranski, *The growth of snow crystals*, *Journal of Crystal Growth* **13**, 236 (1972).
- [5] W. Kingery, *Regelation, surface diffusion, and ice sintering*, *Journal of Applied Physics* **31**, 833 (1960).
- [6] B. Weber, *Sliding Friction: From Microscopic Contacts to Amontons' Law*, PhD thesis, University of Amsterdam, 2017.
- [7] J. M. J. van Leeuwen, *Skating on slippery ice*, 2017.
- [8] A.-M. Kietzig, S. G. Hatzikiriakos, and P. Englezos, *Physics of ice friction*, *Journal of Applied Physics* **107**, 4 (2010).
- [9] P. Oksanen and J. Keinonen, *The mechanism of friction of ice*, *Wear* **78**, 315 (1982).
- [10] S. Calabrese, R. Buxton, and G. Marsh, *Frictional characteristics of materials sliding against ice*, *Lubrication Engineering* **36** (1980).
- [11] D. Slotfeldt-Ellingsen and L. Torgersen, *Water on ice; influence on friction*, *Journal of Physics D: Applied Physics* **16**, 1715 (1983).

- 
- [12] F. Albracht, S. Reichel, V. Winkler, and H. Kern, *On the influences of friction on ice*, *Materialwissenschaft und Werkstofftechnik* **35**, 620 (2004).
- [13] J. J. De Koning, H. Houdijk, G. De Groot, and M. F. Bobbert, *From biomechanical theory to application in top sports: the klapskate story*, *Journal of Biomechanics* **33**, 1225 (2000).
- [14] B. A. Marmo, J. R. Blackford, and C. E. Jeffree, *Ice friction, wear features and their dependence on sliding velocity and temperature*, *Journal of Glaciology* **51**, 391 (2005).
- [15] M. Akkok, McC. Ettles, and SJ Calabrese, *J. Tribol* **109**, 552 (1987).
- [16] D. Evans, J. Nye, and K. Cheeseman, *The kinetic friction of ice*, *Proceedings of the Royal Society of London A: Mathematical, Physical and Engineering Sciences* **347**, 493 (1976).
- [17] L. Bäurle, D. Szabó, M. Fauve, H. Rhyner, and N. Spencer, *Sliding friction of polyethylene on ice: tribometer measurements*, *Tribology Letters* **24**, 77 (2006).
- [18] M. Snijders, *On the presence of a liquid water layer during ice skating*, Bachelor thesis, Leiden University, 2016.
- [19] *Engineering toolbox*.
- [20] R. Fermin, *Assessment of the sub-millimeter structure of ice surfaces during ice skating*, Bachelor thesis, Leiden University, 2015.

# Appendix A: friction measurement parameters

Figure 6.1 shows the information on all measurements used in this thesis, including calculated friction coefficients.

| Filename          | Speed<br>mm/s | Tair<br>C | Tice<br>C | Tskate<br>C | Pressure<br>Bar | Normal force<br>N | Friction force<br>N | Friction coefficient | Comments        |
|-------------------|---------------|-----------|-----------|-------------|-----------------|-------------------|---------------------|----------------------|-----------------|
| From June 2nd     |               |           |           |             |                 |                   |                     |                      |                 |
| 10                | 30            | -10       | -20       | -10         | 3               | 156               | 14                  | 0.08974              |                 |
| 10                | 100           | -10       | -20       | -10         | 3               | 156               | 12                  | 0.07692              |                 |
| 13                | 30            | -10       | -20       | -10         | 3               | 156               | 16                  | 0.10256              |                 |
| 13                | 200           | -10       | -20       | -10         | 3               | 156               | 11                  | 0.07051              |                 |
| 16                | 30            | -10       | -20       | -10         | 5               | 286               | 22.5                | 0.07867              |                 |
| 16                | 100           | -10       | -20       | -10         | 5               | 286               | 17.5                | 0.06119              |                 |
| 19                | 30            | -10       | -20       | -10         | 5               | 286               | 21                  | 0.07343              |                 |
| 19                | 200           | -10       | -20       | -10         | 5               | 286               | 14                  | 0.04895              |                 |
| 36                | 30            | -10       | -20       | -10         | 5               | 286               | 15                  | 0.05245              |                 |
| 36                | 100           | -10       | -20       | -10         | 5               | 286               | 14.5                | 0.0507               |                 |
| 39                | 30            | -10       | -20       | -10         | 3               | 156               | 8                   | 0.05128              |                 |
| 39                | 100           | -10       | -20       | -10         | 3               | 156               | 8                   | 0.05128              |                 |
| 42                | 30            | -10       | -20       | -10         | 5               | 286               | 11.5                | 0.04021              |                 |
| 42                | 100           | -10       | -20       | -10         | 5               | 286               | 11.5                | 0.04021              |                 |
| 46                | 30            | -10       | -15       | -10         | 3               | 156               | 3.5                 | 0.02244              | Tice increased  |
| 46                | 100           | -10       | -15       | -10         | 3               | 156               | 3.5                 | 0.02244              | from -17 to -10 |
| 52                | 30            | -6        | -10       | -10         | 3               | 156               | 1                   | 0.00641              |                 |
| 52                | 200           | -6        | -10       | -10         | 3               | 156               | 1                   | 0.00641              |                 |
| 0                 | 30            | -8        | -10       | -10         | 3               | 156               | 2                   | 0.01282              |                 |
| 0                 | 100           | -8        | -10       | -10         | 3               | 156               | 2                   | 0.01282              |                 |
| 3                 | 30            | -8        | -10       | -10         | 5               | 286               | 3.5                 | 0.01224              |                 |
| 3                 | 100           | -8        | -10       | -10         | 5               | 286               | 4.5                 | 0.01573              |                 |
| 7                 | 30            | -8        | -10       | -10         | 6               | 351               | 4.5                 | 0.01282              |                 |
| 7                 | 100           | -8        | -10       | -10         | 6               | 351               | 5.5                 | 0.01567              |                 |
| --                | --            | --        | --        | --          | --              | --                | --                  | --                   |                 |
| Teflon (June 8th) | 30            | 20        | 20        | 20          | 2               | 91                | 10                  | 0.10989              |                 |

**Figure 6.1:** The parameters and friction coefficients of all measurements done on June 2<sup>nd</sup> and June 8<sup>th</sup>.